19th Annual Meeting of the Bulgarian Section of SIAM
December 11 – 13, 2024
Sofia

BGSIAM'24

EXTENDED ABSTRACTS

HOSTED BY THE JOINT INNOVATION CENTRE
BULGARIAN ACADEMY OF SCIENCES

19th Annual Meeting of the Bulgarian Section of SIAM
December 11 – 13, 2024, Sofia

BGSIAM'23 Extended abstracts

ISSN: 1314-7145 (electronic)

PREFACE

The Bulgarian Section of SIAM (BGSIAM) was formed in 2007 with the purpose to promote and support the application of mathematics to science, engineering and technology in Republic of Bulgaria. The goals of BGSIAM follow the general goals of SIAM:

- To advance the application of mathematics and computational science to engineering, industry, science, and society;
- To promote research that will lead to effective new mathematical and computational methods and techniques for science, engineering, industry, and society;
- To provide media for the exchange of information and ideas among mathematicians, engineers, and scientists.

During the BGSIAM'23 conference a wide range of problems concerning recent achievements in the field of industrial and applied mathematics will be presented and discussed. The meeting provides a forum for exchange of ideas between scientists, who develop and study mathematical methods and algorithms, and researchers, who apply them for solving real life problems.

The strongest research groups in Bulgaria in the field of industrial and applied mathematics, advanced computing, mathematical modelling and applications will be presented at the meeting according to the accepted extended abstracts. Many of the participants are young scientists and PhD students.

LIST OF INVITED SPEAKERS:

- Professor Józef Adam Liwo (Head of Laboratory of Molecular Modeling, University of Gdańsk, Gdańsk, Poland)
  "UNRES Package for Physics-Based Coarse-Grained Simulations of Structure, Dynamics, and Thermodynamics of Protein Systems at Biological Size- and Time Scales"
- Professor Ilian Todorov (Head of the Computational Chemistry Group, STFC Scientific Computing, UK)
  "On the Trail to Exascale & Knowledge Transfer: From the Atomistic to the Mesoscopic World in Preparation for Redox Flow Batteries Modelling"
- Professor Hristo Djidjev (Institute of Information and Communication Technologies, Bulgarian Academy of Sciences, Bulgaria)
  "Beyond Classical Computing: Quantum Approaches to Optimization"

The present volume contains extended abstracts of the presentations (Part A) and list of participants (Part B).

Assoc. Prof. Elena Lilkova
Chair of BGSIAM Section

Prof. Maria Datcheva
Vice-Chair of BGSIAM Section

Assoc. Prof. Todorka Alexandrova
Secretary of BGSIAM Section

Sofia, December 2024

Table of Contents

Part A
Extended abstracts[1]

[1] Arranged alphabetically according to the family name of the first author.

A General Construction of Integer Codes Correcting Specific Bit Errors

T. Alexandrova

Integer codes have been successfully applied to various areas of communication due to their good performance in correcting specific kinds of errors and simple decoding. Very often the used integer code are constructed by computer search.This paper presents an algebraic construction of integer codes over the ring of integers modulo $A = 2^b - 1$. The proposed codes can correct at least up to two bit errors in a single b-byte in a codeword of several b-bytes. Also the codes can correct some configurations of three or more erroneous bits but not all such possible. The proposed construction is based on the use of cyclotomic cosets of 2 modulo A. The simulations of communication through an AWGN channel based on the proposed codes show competitive performance with much simpler decoding in comparison with codes over finite fields.

* * *

Comparison of Two Positivity-Preserving Approaches for Solving Ordinary Differential Equations with Applications to Population Dynamics and Epidemiology

A. Atanasov, S. Georgiev, L. Vulkov

Modelling of real processes by means of differential equations very often requires the positivity of the solutions. At the same time, it is an outstanding problem to develop numerical methods that are both of a higher order of accuracy with preserving positivity. The two main families of numerical methods, Runge-Kutta and multistep methods, face an order barrier, see e. g. [1, Chapter II]. Basic concepts and discretization for ordinary differential equations (ODEs) are discussed in [1, Chapter I]. In this book, Subsection 7.1, the concept for positivity is introduced. Namely, let one write $v \geq 0$ for a vector $v \in \mathbb{R}^m$; if all components are non-negative and consider the ODE system in $\mathbb{R}^m$ for $t \geq 0$: $w'(t) = F\big(t, w(t)\big)$, this system is called *positive* (short for *non-negativity preserving*) if:

$$w(0) \geq 0 \quad \Longrightarrow \quad w(t) \geq 0 \text{ for all } t > 0.$$

Theorem 7.1 provides a simple criterion on F whether the system is *positive*.
The approach in [2] is applied to a large class of ODEs and is based on *graph Laplacian* structure of the system considered. Namely, the authors consider the ODEs:

$$y'(t) = A\big(t, y(t)\big)y(t), \quad y(0) = y_0 \in \mathbb{R}^d, \quad A : \mathbb{R} \times \mathbb{R}^d \to \mathbb{R}^{d \times d}$$

for which the real matrix is graph Laplacian, in particular:

- $A_{kl} \geq 0$ for $k, l = 1, \ldots, d$, $k \neq l$, $\quad A_{kk} \leq 0$, $k = 1, \ldots, d$;
- $\sum_{k=1}^{d} A_{kl} = 0$ for $l = 1, \ldots, d$.

They show cases of applications of their new methods, where standard high-order methods fail to preserve positivity.
In the present work we compare the two approaches on population dynamics and epidemiology including a Susceptible–Infected–Removed (SIR) model [3] and honeybee colony collapse disorder (CCD) model [4].

References

[1] W. Hundsdorfer, J.G. Verwer, Numerical Solution of Time-Dependent Advection-Diffusion-Reaction Equations, Springer, N.Y., (2003).
[2] S. Blanes, A. Iserles, S. Macnamara, Positivity-preserving methods for ordinary differential equations, *ESAIM: M2AN*, 56, 1843-1870, (2022).
[3] S. Georgiev, L. Vulkov, Coefficient identification in a SIS fractional-order modelling of economic losses in the propagation of COVID-19, *J Comput Sci*, 69, 102007 (2023).
[4] A. Atanasov, S. Georgiev, L. Vulkov, Reconstruction analysis of honeybee colony collapse disorder modeling, *Optim Eng*, 22, 2481-2503 (2021).

* * *

The Identification of the Initial Honeybee Density and Fractional Order of a Levy-flight Model to Predict Transgenic Pollen Dispersial

A. Atanasov, M. Koleva, L. Vulkov

The honeybee are responsible for pollinating crops such as blueberris, cherris, and almonds. So, the contaminate of generecally modified (GM) pollen is an issue of significant concern for many countries. For crops that are bee-pollinated, model predictions of outcrossing rates depend on the movement hypothesis use for the pollinators.
Previous papers study pollen spread by honeybees on assuming that the honeybee movement is approximated by Brownian motion. However, recent studies suggest that the pollinating insects such as bees perform Levy flights in their search for food. Such flight patterns yield layer rates of spread, and so the Brownian motion assumption significant underestimated the risk associated with GM pollen outcrossing in conventional crops, described by a space-fractional parabolic equation for the density $B(x,t)$

$$\frac{\partial B}{\partial t}(x,t) = K_\alpha \partial_x^\alpha B(x,t),$$

where $0 < \alpha < 2$ and K_α is the fractional diffusivity.

In the work [1], the authors proposed a mechanistic model for pollen dispersal in which the bees perform truncated Levy flights. We parameterized this model by taking the same pollen dispersal dataset used in Brownian motion modeling studies. Then, we study the inverse problem for identification of honeybee initial density and the the fractional order of the differential operator. Numerical test example with synthetic and real data are presented.

References

[1] V. Valleys, R.C. Tyson, W.D. Lane, E. Deleersnijder, E. Hanet, A Levy-flight diffusion model to predict transgenic pollen dispersal, J. R. Interface 14: 20160889 (2017)

* * *

Parallel Implementations of Modular m-ary Gray Code

D. Bikov, M. Pashinska-Gadzheva, I. Bouyukliev

Gray codes are used in variety of different fields such as digital communications, combinatorics, etc [1–3]. In coding theory, they are used for the computation of weight characteristics of linear codes such as minimal distance, covering radius, coset weight distribution and others, which are computationally heavy problems. The m-ary Gray codes, where $m > 2$, are used for the studying of linear codes over nonbinary finite fields and rings [4–6].
On the other hand, parallelization is one of the more effective ways to target computationally heavy problems, that are hard to solve with standard sequential algorithms. The main goal of this paper is to present optimized and parallelized versions of algorithms for the efficient generation of modular m-ary Gray code and compare the efficiency of the different approaches. We have developed parallel implementations targeting systems with shared and distributed memory with two types of algorithms for generating modular m-ary Gray codes - a version based on the generation of the code as a union of some subsets and a recursive version. The first method is natural and uses an unranking function to partition the set of all codewords into subsets which will be generated in parallel. The second method examines a direct parallelization of a recursive algorithm. The two methods have been implemented with parallel interfaces for shared and distributed memory systems using the Open Multi-Processing interface (OpenMP) and Message Passing Interface (MPI), respectively. The execution times of the presented implementations are compared. Based on the experimental results, we make some observations and conclusions for the efficiency of MPI and OpenMP with recursive and nonrecursive algorithms.

Acknowledgments Partially supported by the Bulgarian National Science Fund under Contract No KP-06-H62/2-2022.

References

[1] C. Savage, “A Survey of Combinatorial Gray Codes”, Siam Rev., 39, pp. 605–629, 1997.

[2] F. Ruskey, Combinatorial Generation. Working Version (1j-CSC 425/ 520). Preliminary Working Draft; University of Victoria: Victoria, BC, Canada, 2003.
[3] Mütze, T. Combinatorial Gray Codes—An Updated Survey. Electron. J. Comb., 30, 2023. .
[4] B.D.Sharma and R.K. Khanna, "On m-ary Gray codes", Information Sciences, vol.15, pp. 31–43, 1978.
[5] M. C. Er, "On Generating the N-ary Reflected Gray Codes," in IEEE Transactions on Computers, vol. C-33, no. 8, pp. 739–741, Aug. 1984.
[6] T. A. Gulliver, V.K. Bhargava and J.M. Stein, "Q-ary Gray codes and weight distributions", Applied Mathematics and Computation, vol. 103, pp. 97–109, 1999.

* * *

Detecting Symmetries via Least-Squares Optimization Algorithms

M. Borisov, S. Harizanov, D. Toneva, S. Nikolova

This paper presents the development of a precise numerical algorithm for the automated detection of the best-fit sagittal plane of a 3D digital human skull model. The algorithm belongs to the group of iterative algorithms for finding the best-fit symmetry plane of a 3D object, but unlike most of them, it is not based on the classical Iterative Closest Point (ICP) algorithm used to minimize the difference between two point clouds. Briefly, the algorithm iteratively solves an optimization problem to find the plane with the smallest asymmetry coefficient, which coefficient represents the Chamfer distance between the one part of the object and the mirror image of the other part, which are obtained by dividing the object into two parts by the plane. As an initial (first) approximation of the best-fit symmetry plane, a plane passing through the center of gravity of the 3D object is taken, with the normal being one of the eigenvectors of the 3x3 Gram matrix generated by the least squares method (LSM). Once an initial plane is obtained, the algorithm begins iterations, and at each iteration, the algorithm attempts to find a plane with a better asymmetry coefficient than that obtained from the previous iteration by rotating and translating the plane from the previous iteration. The iteration continues until the best-fit symmetry plane is found, i.e., until the planes obtained at the end of two consecutive iterations have "equal" (within a predefined tolerance) asymmetry coefficients. Additionally, the algorithm's results on 14 digital human skull models, obtained from computed tomography, are presented and compared with the results obtained using landmark points manually selected by an expert.

Acknowledgments This work is supported by the Bulgarian National Science Fund, Grant number KP-06-H51/4–11.11.2021.

* * *

Numerical Simulation Strategy for Nanoindentation Testing of Thin Films

G. Chalakova, M. Datcheva, R. Iankov

Numerical modeling of the nanoindentation process provides a powerful method to study the mechanical properties of thin films, such as hardness, elastic modulus, and yield strength, taking into account the influence of the substrate and indentation parameters. Using a finite element analysis (FEA) tool, such as Abaqus, it is possible to reproduce experimental setups and investigate the mechanical behavior of materials under controlled conditions.

The nanoindentation process involves applying a load to an indenter that penetrates a thin film while monitoring the load and displacement. Simulation aims to reproduce this interaction using numerical models. Abaqus is the tool of choice due to its robust non-linear solver, adaptive mesh, and ability to model complex material behavior such as elastic-plastic transitions.

In this study Pd–In alloy films with thickness between 0.6 and 3.8 μm were deposited onto brass sheet substrates (2x1x0.03 cm). Their mechanical properties (hardness and indentation modulus) were then determined using Nanoindenter G200 (Keysight Technologies) equipped with a standard XP indenter head, which allows for measurements with depth accuracy of $< 0.01nm$ and applied load accuracy of 50 nN. The indenter head is equipped with Berkovich tip (sharp diamond three-sided pyramid). The main goal was to assess the effect of chemical and phase composition, as well as structure of the films, on the mechanical properties (indentation hardness and modulus) of the investigated Pd–In thin films regardless of the difference in the thickness and the significance of the surface roughness. It has been demonstrated that the mechanical properties of these films are highly compositionally sensitive, and the surface roughness yields scatter in the results and introduces uncertainty in the obtained mechanical characteristics [1].

During thin coatings nanoindentation, roughness is a serious factor affecting the results obtained within mechanical tests. In relation to the conducted experiments, two different approaches to modeling the nanoindentation process are considered. In one case, the possibility of incorporating surface roughness into the sample is explored using the method outlined in [2]. In the other case, a regression method is examined with the aim of eliminating errors caused by morphology, as proposed in [3].

During the numerical simulation, the investigated Pd-In thin films are modeled as anisotropic elastic-plastic materials. The brass substrate is treated as an elastic material. The Berkovich indenter tip is modeled as a rigid body to simplify computations.

References

[1] G Chalakova et al. “Nanomechanical testing of thin composite layers–Application to Pd-In electrochemically deposited thin films”. In: AIP Conference Proceedings. Vol. 1684. 1. AIP Publishing. 2015.

[2] Youngbin Lim and Sangyul Ha. “RufGen: A plug-in for rough surface generation in Abaqus/CAE”. In: SoftwareX 22 (2023). ISSN : 2352-7110. DOI: 10.1016/j.softx.2023.101380.

[3] Xiaozhen Li et al. “Numerical Study on the Regression Method to Eliminate the Influence of Surface Morphology on Indentation Hardness of Thin Films”. In: Coatings 12.10 (2022). ISSN : 2079-6412. DOI: 10.3390/coatings12101447.

* * *

Beyond Classical Computing: Quantum Approaches to Optimization

H. Djidjev

Classical computers struggle with many optimization challenges, from molecular modeling to resource scheduling. Quantum annealing computers (QACs), such as those developed by the Canadian company D-Wave Systems Inc., utilize quantum effects to search for solutions to such challenging optimization problems. Unlike the more well-known universal quantum computers, QACs are specialized for dealing with a class of problems known as quadratic unconstrained binary optimization (QUBO), a framework that efficiently represents many NP-hard problems. Thanks to this specialization, these computers feature a much larger number of qubits compared to existing universal quantum computers and offer streamlined programming interfaces for optimization tasks. This is especially useful because many important NP-hard problems—such as the maximum clique problem, graph coloring, and the maximum cut problem—can be naturally formulated as QUBOs.
In this talk, I will provide a brief overview of quantum computing fundamentals, followed by a more detailed discussion of QAC architecture and operation. Using examples from combinatorial optimization, I will demonstrate key methods and discuss current technical challenges in using QACs, along with some techniques to overcome these limitations.

* * *

Exact Real Computer Arithmetic: A Study from an Information Theory Perspective

J. Genoff

The simple sad truth that real numbers in general have infinite range and accuracy makes the efforts to represent them and operate on them in the contemporary binary von Neumann computer, which is finite in any aspect, almost a chimera. Numerous workarounds have been in development for decades and each one struggles for the optimal compromise amidst the triangle of representation space (denoted as precision), operations execution time (a.k.a. performance) and numeric accuracy and/or range.

This study aims to devise a specific compromise approach. It is based on the notion that every number can be viewed as a message, carrying certain amount of information. Real numbers in general carry infinite amount of information. Any finite representation, as in the computers, is a finite length message with a finite amount of information. The different models of number representation utilize the message capacity in different ways, hence the different degree of inaccuracy, i.e. error introduced in the representation. If a requirement constraint exists on the representation space size, then the choice of the best model of representation can be crucial, especially when the model must be changed during the computation, in order to maintain the highest accuracy.

The core of this research investigates the ability of several models to achieve maximum accuracy at the same message length. The standard floating-point format is chosen as a pivot model for its simplicity of representation and easy parameter manipulation. In order to estimate the accuracy of some of the other models in consideration, a ("source") numeric value is represented as a number by this ("source") model and the representation is assumed to be an exact real number. Then the same numeric value is represented as a ("pivot") floating-point number, whose overall representation length is constrained to be the same as the source model representation length. This constraint is actually achieved by applying floating-point rounding, which in general introduces a rounding error. Finally, the relative error between the source and the pivot representations is determined, and this error is considered an estimation of the inaccuracy of the pivot model in comparison to the source one. The higher the error, the better the information capacity of the source model representation is utilized. Subjecting each of the models to this procedure and using the same source numeric value, but striving for the optimal number representation by each of them, it is possible to assess which model has the highest information carrying capacity.

Here all number representations are considered binary and optimal in the sense that all the available mathematical background of the given model is utilized at its maximum to achieve shorter message, and moreover, the information theory concept of information being eliminated uncertainty is applied to produce minimal-length messages. The relative error for inaccuracy estimation ca be determined in two ways: an exact one, doing exact arithmetic on the finite length source model number and the finite length pivot floating-point number; and a simpler one, doing floating point arithmetic on two versions of the pivot floating point representation – the one with the exact same message length as the source model representation and one with a longer length, as much as more precise estimation of the error is needed.

Among the numerous exact real number models, this study focuses on some of the most straightforward ones: fractions of floating-point numbers; floating-point numbers, whose significands are simple fractions of integers; and floating-point numbers whose significands are continued fractions of integers. Besides, the study extends to models that are not so much exact, but are widely adopted for the so called "verified" computing: interval arithmetic numbers and ball arithmetic numbers.

Since the formal error bounds for the described source-pivot accuracy estimation are not yet derived, this paper presents many numeric experimental results that give a clear idea of the importance of the approach considered above.

* * *

Evaluation of the Binding Free Energy of Peptide Complexes Using Machine Learning

V. Ivanova, P. Petkov, E. Lilkova , L. Litov, N. Ilieva

Protein-protein and protein-peptide interactions (PPIs) are central to numerous critical cellular processes. A thorough understanding of these interactions is vital for elucidating cellular mechanisms and plays a pivotal role in the development of drugs designed to regulate them [1].

The investigation of PPIs is inherently challenging, as traditional experimental methods are both time-consuming and resource-intensive. To address these challenges, machine learning (ML) and artificial intelligence (AI) models have been employed to identify binding sites on target proteins and estimate ligand binding affinity, often utilizing scoring functions [2]. Among these, convolutional neural networks (CNNs) have emerged as the most reliable and widely used frameworks [3].

A more targeted strategy for studying PPIs involves determining the binding energy of protein-peptide complexes. While numerous ML models exist for predicting various attributes of protein complexes, none are currently recognized as dependable for accurately estimating the binding energy of interacting biomolecules.

In this work, we propose a novel approach that digitizes the three-dimensional structural data of protein-protein and protein-peptide complexes. Additionally, we introduce a minimal convolutional network architecture that demonstrates significant potential for accurately predicting the binding energy of these molecular complexes.

Acknowledgments This research is partially funded by the Bulgarian National Science Fund under contract KP-06-N72/3/2023 AIDA.

References

[1] Garrett, R. H., & Grisham, C. M. Biochemistry (5th ed.). Brooks/Cole, Cengage Learning, (2013)

[2] Yin S, Mi X, Shukla D. Leveraging Machine Learning Models for Peptide-Protein Interaction Prediction, Chem Biol. 5(5), 401-417 (2024)

[3] Marta M. Stepniewska-Dziubinska Piotr Zielenkiewicz and Pawel Siedlecki. Development and evaluation of a deep learning model for protein-ligand binding affinity prediction, Bioinformatics, Volume 34, Issue 21, 3666–3674 (2018)

* * *

Using EOS Blockchain for Verifiable Random Number Generation with User-Contributed Entropys

J. Jeliazkov, H. Kostadinov

This article describes a prototype decentralized application (dApp) designed to generate verifiable random numbers using the EOS blockchain and its future block hashes. The dApp allows competing parties to contribute to the random number generation (RNG) process by submitting the hash of a secret number, which they reveal after a specific block is mined. By combining the unpredictable nature of future block hashes with user-contributed entropy, the dApp ensures randomness that is unbiased and tamper-resistant. The entire process, from hash submission to secret disclosure to final RNG calculation, is recorded on the blockchain, ensuring transparency and verifiability. This prototype highlights the potential of blockchain technology to create secure, decentralized randomness for various applications.

References

[1] Choi K., Manoj A., Bonneau J.: SoK: Distributed Randomness Beacons. IEEE Symposium on Security and Privacy, (2023).

[2] Micali S., Rabin M., Vadhan S.: Verifiable random functions. Annual IEEE Symposium on Foundations of Computer Science, (1999).

[3] Luu L., Narayanan V., Zheng C., Bajewa K., Gilbert S., Saxena P.: A Secure Sharding Protocol for Open Blockchains. Proceedings of the 2016 ACM SIGSAC Conference on Computer and Communications Security, 17-30 (2016).

[4] Cachin C., Kurwase K., Shoup V.: Random oracles in constantipole: practical asynchronous byzantine agreement using cryptography. Proceedings of the nineteenth annual ACM symposium on Principles of distributed computing, 123-132 (2000)

* * *

First Remarks on Scaling Theory of Spread of COVID-19 in Bulgaria

S. Kartalov, N.K. Vitanov

We discuss the application of the allometric scaling analysis method for the purpose of analyzing the dynamics of the spread of the COVID-19 pandemic. The possibility for the application of this methodology is based on the assumption that the vulnerability of the urban system to the COVID-19 pandemic is its property, based on the social connections and relations that define it, and therefore manifests itself in a physically similar scale-invariant manner. This scale-invariance is both in terms of physical space and in terms of physical time. This assumption was very recently confirmed by the analysis of real-time empirical data on the dynamics of the spread of COVID-19.

By combining the ideas of scale-invariance and self - similar system behavior, we arrive at the idea and hypothesis of a transition from static to dynamic scaling analysis. The dynamic scaling unites in its classical definition system characteristics related to the spatial distribution of the growth of the system and its parts, as well as those related to its behavior over time.
By analogy with the process of mass transmission in the system (diffusion), we assume that for the entry and spread of COVID-19 in the urbanized system it is possible to introduce a criterion and number of similarity (homochrony). When describing the dynamics of each separately taken subsystem of the national system (at the level of NUTS3 regions), we assume that for the considered periods the changes in the population number in it are small and the corresponding population, N is constant over time. In each case, the cumulative number of established cases increases as a power function of relative time. The scale of increase is determined by the value of the power function of the population simplex for each of the subsystems (populations), as well as by the average value of the cumulative number of established cases of COVID-19 after a certain, characteristic for a given subsystem, time has elapsed.
The application of the scaling theory allows us to study numerous aspects of the spread of COVID-19 disease in Bulgaria. Some of the obtained results will be presented and discussed.

* * *

Minimizing the Number of Questions in Test Examinations with Genetic Algorithms Without Loss of Test Sensitivity

D. Keremedchiev, T. Balabanov

Using a predefined set of possible answers for testing is widespread and well-received. Therefore, it is essential to optimize the testing process. The examiner should be able to thoroughly assess the examinees while ensuring they do not feel pressured. Shorter questionnaires sensitive to the examinees' skills and knowledge can meet both these requirements.

When setting the available time for the exam, consideration must be given to time constraints. Balancing the time allotted for examinees to read and respond to each question within the allocated timeframe is crucial. The exam content should also cover the material taught in the course or lesson. The number of questions should be sufficient to evaluate students' comprehension of key concepts and topics. As a general guideline, exams with closed questions often comprise around 20 to 50 questions, varying based on different factors.

The sensitivity of a closed-answer test depends on its ability to measure differences in knowledge or understanding among test-takers accurately. The number of questions significantly influences the impact of the test's sensitivity. Increased precision is achieved by raising the number of questions and improving sensitivity. This improvement is due to the broader assessment of the test-taker's knowledge or abilities facilitated by more questions. Additionally,

more questions enable a more comprehensive evaluation of individual differences and reduce sampling errors driven by random variability. With more questions, the impact of random guessing or chance fluctuations in performance is minimized, resulting in more reliable and precise results. Moreover, more questions enhance discrimination between high-performing and low-performing individuals, contributing to more accurate rankings or classifications of individuals based on their test performance. However, it is worth noting that increasing the number of questions means longer exams and higher resource usage.

The optimal number of questions for an exam with closed questions depends on various factors, such as the complexity of the material being assessed, the time allotted for the exam, and the desired level of detail in evaluating students' understanding. Test sensitivity is strongly correlated with the number of questions in the questionnaire; therefore, the number of questions is crucial for test measurement quality. Lastly, a bank of questions can be used for test assembling, and genetic algorithms can be helpful for this purpose.

* * *

High-Order Difference Schemes for Quasilinear Pseudo Parabolic Equations

M. Koleva, L. Vulkov

Motivated by Aller-Lykov equation:

$$\frac{\partial u}{\partial t} = \frac{\partial}{\partial x}\left(a(u)\frac{\partial u}{\partial x}\right) + \varepsilon\frac{\partial^3 u}{\partial t \partial x^2}, \;\; \varepsilon > 0,$$

our basic interest in this paper is the 1D pseudoparabolic equation

$$\frac{\partial u}{\partial t} = \frac{\partial}{\partial x}\left(a(u)\frac{\partial u}{\partial x} + b\left(\frac{\partial u}{\partial t}\right)\frac{\partial^2 u}{\partial t \partial x}\right) \;\; \text{in} \;\; Q_T = (0,1)\times(0,T), \tag{1}$$

subject (1) with initial and boundary conditions:

$$u(x,0) = u_0(x), \;\; x \in (0,1), \;\; u(0,t) = u(1,t) = 0, \;\; t \in [0,T]. \tag{2}$$

We introduce the uniform mesh $\overline{w}_{h\tau} = \overline{w}_h \times \overline{w}_\tau$, where

$$\overline{w}_h = \left\{x_i = ih, \; i = 0,1,\ldots,I, \; h = \frac{1}{I}\right\}, \; \overline{w}_\tau = \left\{t_j = j\tau, \; j = 0,1,\ldots,J, \; \tau = \frac{T}{J}\right\}.$$

We rewrite the equation (1) in the form

$$\frac{\partial u}{\partial t} = \frac{\partial^2}{\partial x^2}\left(A_1(u)\right) + \frac{\partial^2}{\partial x^2}\left(B_1\left(\frac{\partial u}{\partial t}\right)\right),$$

$$(A_1(u))' = a(u), \quad \left(B_1\left(\frac{\partial u}{\partial t}\right)\right)' = b\left(\frac{\partial u}{\partial t}\right).$$

Using second-order difference derivative approximation, we have

$$\begin{gathered}(A_1(u))_{\overline{x}x,i} = \frac{\partial^2}{\partial x^2}\,(A_1(u))|_{x=x_i} + \frac{h^2}{12}\frac{\partial^4}{\partial x^4}\,(A_1(u))|_{x=x_i} + O(h^4),\\ \left(B_1\left(\frac{\partial u}{\partial t}\right)\right)_{\overline{x}x,i} = \frac{\partial^2}{\partial x^2}\left(B_1\left(\frac{\partial u}{\partial t}\right)\right)_{x=x_i} + \frac{h^2}{12}\frac{\partial^4}{\partial x^4}\left(B_1\left(\frac{\partial u}{\partial t}\right)\right)_{x=x_i} + O(h^4).\end{gathered} \tag{3}$$

Using the averaging

$$k(u(x,t)) \approx \frac{1}{\widehat{u}-u}\int_u^{\widehat{u}} k(u)du, \quad u = u(x,t^j), \quad \widehat{u} = u(x,t^{j+1}), \quad y_t = \frac{\widehat{y}-y}{\tau},$$

we approximate the left-hand side of (3) as follows:

$$\begin{gathered}(A_1(u))_{\overline{x}x,i} \approx \left(\frac{A_2(\widehat{u}) - A_2(u)}{\widehat{u}-u}\right)_{\overline{x}x,i}, \quad A_2(u) = \big(A_1(u)\big)',\\ \left(B_1\left(\frac{\partial u}{\partial t}\right)\right)_{\overline{x}x,i} \approx \left(\frac{B_2\left(\frac{\partial \widehat{u}}{\partial t}\right) - B_2\left(\frac{\partial u}{\partial t}\right)}{\frac{\partial \widehat{u}}{\partial t} - \frac{\partial u}{\partial t}}\right)_{\overline{x}x,i}, \quad B_2\left(\frac{\partial u}{\partial t}\right) = \left(B_1\left(\frac{\partial u}{\partial t}\right)\right)'.\end{gathered} \tag{4}$$

We differentiate the equation (1) two times with respect to x to find:

$$\left.\frac{\partial^3 u}{\partial t \partial x^2}\right|_{x=x_i} = \left.\frac{\partial^4}{\partial x^4}(A_1(u))\right|_{x=x_i} + \left.\frac{\partial^4}{\partial x^4}\left(B_1\left(\frac{\partial u}{\partial t}\right)\right)\right|_{x=x_i}. \tag{5}$$

From (3)-(5) we obtain the following $O(h^2+\tau^2)$ -order approximation of (1):

$$y_t + \frac{h^2}{12}y_{\overline{x}xt} = (A_2(\widehat{y},y))_{\overline{x}x} + (B_2(\widehat{y}_t,y_t))_{\overline{x}x}.$$

In a similar way, one can derive $O(h^2+\tau^{2-\alpha})$ accurate difference schemes for time fractional α - order PDEs as well as to 2D equations.
Further, in combination with approximation of (2) and Newton or Picard iterations, we solve the nonlinear algebraic systems of equations on each time layer.

* * *

Digital Twin of Solar PV Panel Clamping

Y. Madankov, R. Iankov

This work aims to develop and verify an adequate and robust numerical model as a step toward creating a digital twin for studying a specific type of photovoltaic panel fastening system, which has demonstrated imperfections under certain wind load conditions. A comprehensive numerical simulation model is proposed to analyze the stress-strain behavior of the fastening system, enabling the evaluation of its performance and potential failure modes. The next objective is to identify specific wind load conditions that could lead to potential weaknesses and assess corresponding failure scenarios. The simulation results confirm the likelihood of failures in the fastening elements under these conditions.
By integrating numerical simulation methods, the model serves as a foundation for a dynamic and interactive representation of the fastening system, with the potential to incorporate real-time data for enhanced predictive capabilities. The finite element method (FEM) was employed to perform these simulations, ensuring detailed and accurate analysis. This study lays the groundwork for the development of a fully functional digital twin in future research efforts.

* * *

A Probabilistic AI Model Implementation with the Future Complex Cybersecurity Systems

Z. Minchev, S. Tafkov

Modern cybersecurity systems are naturally evolving with the mass digitalization of the new cyber-physical world, getting constant complexity growth [1]. At the same time this naturally creates numerous cybersecurity threats and challenges that have to be successfully tailored [2]. In this sense, it is important to note that the implementation of AI algorithms in this field is quite useful, taking both offensive & defensive perspectives. What however is important to add here is the possibility for successful prediction and respective defense of potential hostile activities towards future complex cybersecurity systems development with multiple smart applications (infrastructure handling, production & entertainment systems or other suitable services with the newly transformed digital reality). Another key moment is the speed of the responsive AI algorithms handling these tasks [3]. The study presents a conceptual AI probabilistic model, based on switching thresholds & quantum tunneling ideas [4], that is practically implemented with a cybersecurity protection system prototype, producing real information resources and infrastructure security handling [5]. Further on, some experimental data is provided, giving an experimental assessment of the effectiveness of the proposed ideas with the new digital reality.

Acknowledgments The study is partially supported with National Scientific Program "Security & Defence". Additional gratitude for the expert & collaborative support is given to Secure Digital Future 21 initiative & EDIH Trakia.

References [1] Minchev, Z., et al. Digital Transformation in the Post-Information Age, Institute of ICT & SoftTrade, 2022
[2] 2024 Data Breach Investigations Report, Verizon, 2024. [Online].
https://www.verizon.com/business/resources/reports/dbir/. [Accessed: 1-Dec-2024].
[3] Misra, S., Tyagi, A. (Eds) Artificial Intelligence for Cyber Security: Methods, Issues and Possible Horizons or Opportunities, Studies in Computational Intelligence, Springer, 2021
[4] M. Razavy, Quantum Theory of Tunneling, 2nd Edition, World Scientific, 2014
[5] Tafkov, S. Adaptive Measurement Systems with ML for End-point Protection, Stefan Tafkov, Jubilee International Seminar "The Role of Information Technologies in Security & Defence: Capacity & Development Perspectives for Bulgaria in Regional & Global Partnership Context", IT for Security Department, AOR "Atlantic", Central Military Club, Sofia, November 25, 2024

* * *

A 3D-SNN Brain Model

S. Nedelcheva

A 3D spike timing neural network model of brain was designed using Desikan-Killiany atlas. It was designed using in NEST Simulator library. The connectivity within the 3D-SNN was created based on distances between each to neurons and their strength decrease exponentially with increase of distance. Simulation results demonstrate how the sensory input information spreads through the designed 3D-SNN structure.

* * *

Variance-based Sensitivity Analysis of the Unified Danish Eulerian Model with Using a Robust Monte Carlo Simulation Approach

T. Ostromsky, V. Todorov

This work conducts a detailed variance-based sensitivity analysis using the Unified Danish Eulerian Model (UNI-DEM), a sophisticated air pollution model designed to simulate the dispersion and transformation of atmospheric pollutants across Europe and neighbouring regions. Its numerical calculation requires great computational power and smart parallel algorithms. This is a challenging problem even for the largest and fastest supercomputer systems

nowadays. Fortunately, Bulgaria became one of the leading European countries with regard to the supercomputer infrastructure development in the recent years. This study strongly relies on the experiments carried on the supercomputer Discoverer. It is the third Bulgarian supercomputer ranked in the list of the TOP 500 most powerful supercomputers in the world, as well as the first with computational speed exceeding one PFlops in the Balkan region.
By using a robust Monte Carlo simulation approach, we evaluate the influence of various input parameters, such as emission rates of various groups of pollutants, meteorological data, and chemical reaction rates on the output concentrations of key airborne pollutants. Our analysis leverages Sobol' sensitivity indices to quantify both main and interaction effects of these variables, providing insight into the predominant factors that impact air quality. This research not only deepens our understanding of the complex dynamics governing air pollution, but also aids in crafting precise environmental policies by pinpointing the most effective areas for regulatory action. The results highlight critical drivers of air quality variations and support targeted interventions to improve air pollution control measures, utilizing the comprehensive capabilities of the UNI-DEM. This study would hopefully serve as a significant step towards optimizing air quality management strategies and developing more sustainable environment.

Acknowledgments This research was supported in part by the Bulgarian NSF project "Efficient methods for modelling, optimization and decision making" (contract # KP-06-N52/5), as well as by the Petascale-Bulgaria Supercomputer Consortium and EuroHPC Joint Undertaking.

* * *

The Complex Study of the Anthropogenic Influence on the State of the Atmosphere and Hydrosphere

M. Petrov, V. Traneva, S. Tranev, V. Todorov, S. Georgiev

The study of the state of the hydrosphere of the oceans under the influence of anthropogenic gases accumulated in atmosphere with greenhouse effect (especially carbon dioxide) is the current major task of whole World. Previous studies showed that carbon dioxide has the major effect of the order of 75% from all green house gases of the atmosphere [1]. This recent study aims to develop the qualitative and quantitative description of the oceans with the application of the results of the suggested method of the paper [1]. A series of papers describe the acidification of ocean waters as a result of the absorption of carbon dioxide from the atmosphere. The value of pH of ocean waters tends to decrease (becomes much more acidic) [2]. Seawater pH has decreased from 8.11 in 1985 to 8.05 in 2021. (Fig. 1) [3]. The source [4] describes the role of phytoplankton and the period of the year 1994 is characterized by the level of 40-50 Gt/year of the utilization of carbon dioxide for the

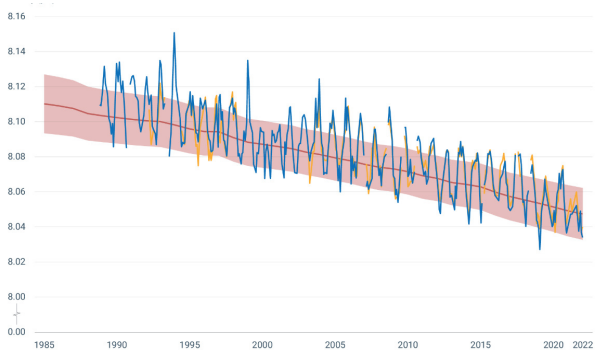

Figure 1: Decline in ocean pH on a global scale [3].

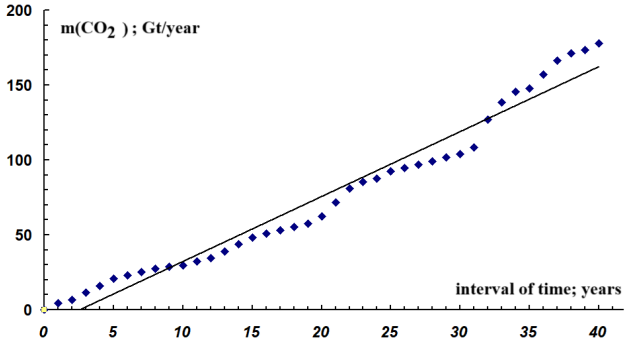

Figure 2: The quantity of carbone dioxide used by the ocean's phytoplankton.

production of oxygen. Nowadays the production of oxygen by phytoplankton is almost 50% of total produced oxygen [5].

The main result is the procedure of the calculation of the carbon dioxide used by ocean's phytoplankton and this result is of the order 178 Gt/year. Such quantity of $CO_[2]$ produces $O_[2]$ of the order 130 Gt/year from the total oxygen 293 Gt/year (Fig. 2), (Fig. 3).

The paper [6] appreciates the vital role of phytoplankton in sustaining life on Earth and the necessity to protect these tiny creatures that make our planet habitable.

References

[1]Petrov, M.: Major contribution of carbon dioxide excess in atmosphere to the green house effect. Oxidation Communications **44** (4), 870–907 (2021). https://scibulcom.net/en/journal/0209-4541/issue/2021-44-4/

[2] Fabry, V. J., Seibel, B. A., Feely, R. A., Orr, J. C.: Impacts of ocean acidification on marine fauna and ecosystem processes. ICES Journal of Marine Science **65** (3), April 2008, 414–432 (2008). https://doi.org/10.1093/icesjms/fsn048

[3] Ocean acidification. https://www.eea.europa.eu/en/analysis/indicators/ocean-acidification#: :

[4] Falkowski, PG. The role of phytoplankton photosynthesis in global biogeochemical cycles. Photo-

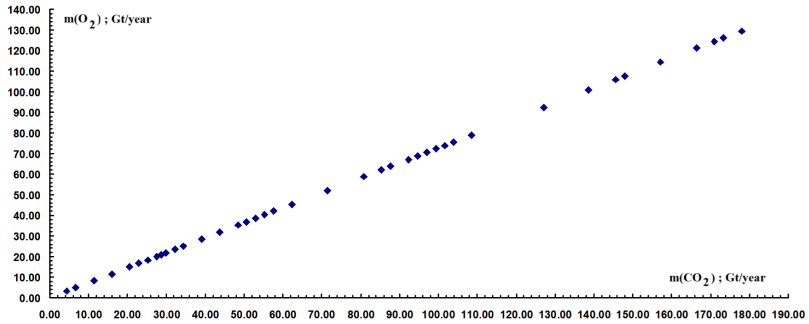

Figure 3: The production of oxygen by ocean's phytoplankton.

synth Res.**39** (3), 235-58 (1994). doi: 10.1007/BF00014586. PMID: 24311124.
[5] How much oxygen comes from the ocean? https://oceanservice.noaa.gov/facts/ocean-oxygen.htm
[6] Phytoplankton: The Unseen Heroes of Oxygen Production. https://www.therokter.com/aquaculture-blog/phytoplankton-heroes-of-oxygen production

* * *

Numerical simulation of thermal stratification in underground long-term hot water storage. Effects of the aspect ratio

M. Rashevski, M. Datcheva, S. Slavtchev

A two-dimensional analysis of the thermal losses in underground long-term hot water storage of rectangular shape over 180 days is reported. Three different aspect ratios (AR) are considered: $AR = 4, AR = 1, AR = \frac{1}{4}$, but with the same enclosed area (Fig. 1).
The mathematical model is based on the unsteady Navier-Stokes-Fourier equations with Boussinesq approximation, expressed in their vorticity-stream function form. The storage is represented by a closed symmetric rectangular cavern with plane walls and uniform initial temperature which gradually cools down over the studied period of time. The temperature conditions on the walls model the heat transfer through the storage boundaries evolving in a way described in details in [1]. Finite difference method (FDM) is used to obtain numerical solutions. Graphical results for the stream lines (Fig. 2a) and temperature distribution (Fig. 2b) are plotted at the final time step. Finally, some important thermal characteristics such as the thermocline thickness (Fig. 3) and the Nusselt number on the cavern walls are evaluated.

The results show that the vortices in the quadratic and shallow tank geometries entrain larger fluid volumes and contribute for stronger mixing processes and for less pronounced thermal

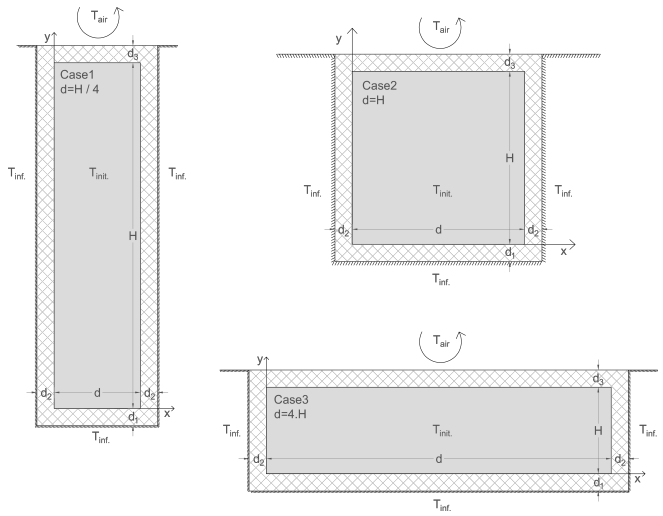

Figure 1: Geometries of the underground hot water storage at the initial state $t = 0$

stratification. The vertical narrow storage on the other hand has the highest mean fluid temperature and the highest temperature difference between the cold and hot fluid areas. These results indicate the benefits of the latter design in respect to its accumulation capacity and energy efficiency which may be compared in future works to the expected over cost for deeper excavation works.

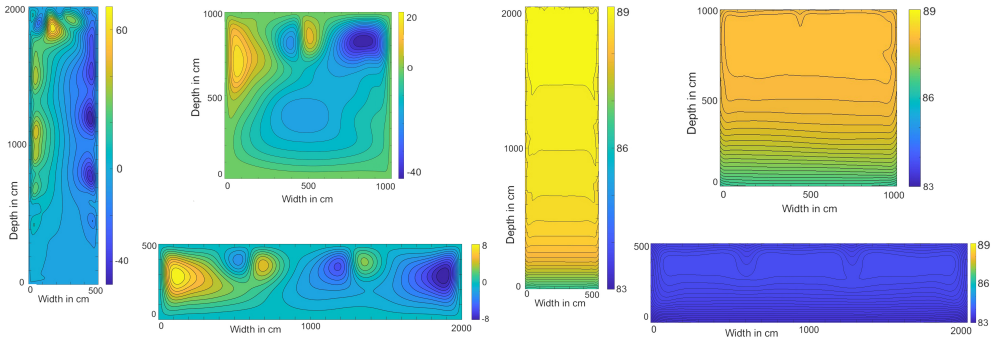

(a) (b)

Figure 2: Stream lines (2a) and temperature fields (2b) for the three cases under consideration

Acknowledgments This work was supported by the Next Generation EU program, project number BG-RRP-2.017-0036 “Seasonal and short-term thermal energy storage systems with

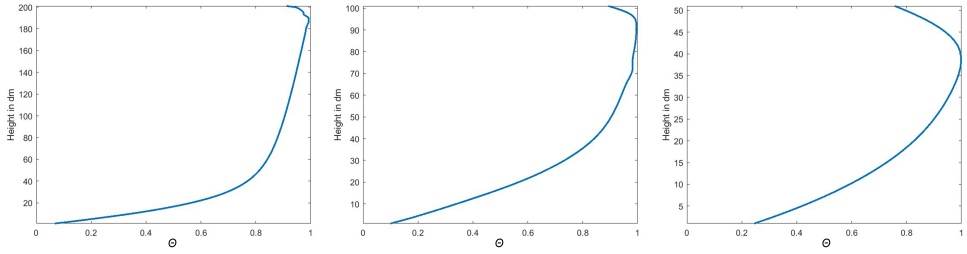

Figure 3: Vertical temperature profiles in the middle section of the storage for $AR = 4, 1$ and $\frac{1}{4}$ (from left to right).

geothermal heat exchangers and phase change materials, using renewable energy sources".

References

[1] Rashevski, M., Slavtchev, S.: Convective thermal losses of long-term underground hot water storage. J. of Therm. Eng. 10(2), 490–502 (2024).

* * *

A General Construction of Integer Codes Correcting Specific Bit Errors

M. Raykovska, I. Georgiev, M. Mourdjeva

In case of damage or a medical condition affecting the skull, surgery is often required to reconstruct cranial defects. This is usually done using synthetic bone replacement materials or autografts. By creating models of large-scale calvarial defects, we can evaluate the regenerative properties of various biomaterials, growth factors, progenitor cells, and epigenetic drugs. The calvarial defect model is helpful in studying bone healing in a clinically relevant and orthotopic setting.

BV/TV (Bone Volume Fraction or Tissue Volume Fraction) is a quantitative metric commonly used in bone tissue engineering and medical imaging studies. It represents the ratio of the volume of bone to the total volume within a defined region of interest. BV/TV is crucial in assessing bone density and structure, and it helps researchers and clinicians quantify changes in bone structure due to disease, aging, or other factors. BV/TV is a crucial parameter in bone regeneration, tissue engineering, and bone health assessment

One of the main challenges in examining in vivo groups is the inherent variability in their growth rates. Even mice from the same genetic lineage can have different growth trajectories, which affects both their preoperative bone volume and the regenerative processes that follow the induction of bone defects. Therefore, it's important to establish a robust methodology that allows for individualized comparison of bone volume ratios for each mouse. This

study aims to propose and explain a method for normalizing examined specimens, which addresses the complexities posed by disparate growth dynamics among mice. By mitigating the confounding impact of variable growth rates, this methodology can increase the precision and reliability of comparative analyses, thereby contributing to the methodological refinement of studies in murine calvarial defect modeling.Overall, this study's proposed method for normalizing examined specimens will help researchers obtain more precise and reliable results when studying groups of mice, and ultimately advance our understanding of bone growth and recovery processes.

* * *

Utilizing open-source toolkits for avalanche formation and space-charge effects in Resistive Cylindrical Chambers

E. Shumka, P. Petkov, B. Pavlov, A. Petrov, M. Pehlivanova

Resistive Cylindrical Chambers (RCC) have been introduced in recent years as an innovative approach to constructing resistive gaseous detectors. This design offers the advantage of a robust mechanical structure capable of withstanding higher gas pressures, thereby enhancing efficiency. Additionally, the inhomogeneous electric field inherent to this geometry improves avalanche containment, reducing the likelihood of streamers.
Simulating avalanche formation and space-charge effects in RCC is crucial at this stage of their development. These simulations allow for a thorough investigation of the detector's properties and help verify whether the proposed advantages are realized in this novel geometry.
Here, we present a unified interface for conducting all simulation steps using open-source tools. This approach includes enhancements such as parallel execution with MPI and integration of alternative finite-element method (FEM) software, such as FEniCSx, alongside the established Garfield++ simulation package.

Acknowledgments The research is partially funded by the European Union - NextGenerationEU, through the National Recovery and Resilience Plan of the Republic of Bulgaria, project SUMMIT BG-RRP-2.004-0008-C01.

* * *

Conformational dynamics of the cysteine knot motif in native and grafted cyclotides from trypsin inhibitor family

P. Sirakova, P. Petkov, E. Lilkova, N. Ilieva, L. Litov

Peptide aptamers, small proteins capable of binding to variety of target molecules, hold significant potential for modulating or inhibiting these targets [1]. Their binding affinity is closely tied to their conformational flexibility: while flexibility enables adaptation to target surfaces, restricting their conformational ensemble can enhance binding affinity by reducing the entropic contribution. One approach to achieve such conformational constraint is to graft peptide aptamers onto protein scaffolds, which stabilizes their desired conformation [2].
Cyclotides, a family of cyclic peptides, are exceptional scaffolds for this purpose due to their remarkable stability and structural diversity [3]. These miniproteins feature a head-to-tail cyclized backbone and a cystine knot motif (CKM) formed by three interlocking disulfide bonds, providing both robustness and adaptability. Grafting involves embedding the peptide aptamer sequence into one of the cyclotide's loop regions without compromising its structural integrity. Successful cyclization and folding of the grafted cyclotides are critical to the production of bioactive molecules that retain the stability and functionality of the cyclotide scaffold [4].
In this study, we explore the use of molecular modeling to select grafted cyclotides with functional structures. Specifically, we investigate the interactions between the native cyclotide MCoTI-I and its target, trypsin, to understand how binding affects the stability and conformation of the CKM. The goal is to demonstrate that binding to trypsin provides a framework for identifying grafted cyclotide topologies with proper folding and cyclization patterns, paving the way for the development of functional bioactive molecules.

Acknowledgments This research was partially supported by the Bulgarian Science Fund under Grant KP-06-N71/3/2023 AVATAR.
Computational resources were provided by CI TASK (Centre of Informatics–Tricity Academic Supercomputer & networK), Gdansk (Poland), as well as the BioSim HPC cluster at the Faculty of Physics, Sofia University "St. Kliment Ohridski".

References

[1] Sergey Reverdatto, David S. Burz, and Alexander Shekhtman. Peptide aptamers: de- velopment and applications. *Current topics in medicinal chemistry*, 15(12):1082–1101, 2015.
[2] Krištof Bozovičar and Tomaž Bratkovič. Small and simple, yet sturdy: conformation- ally constrained peptides with remarkable properties. *International journal of molecular sciences*, 22(4):1611, 2021.
[3] Andrew Gould and Julio A Camarero. Cyclotides: overview and biotechnological applications. *ChemBioChem*, 18(14):1350–1363, 2017.
[4] Michelle L Colgrave and David J Craik. Thermal, chemical, and enzymatic stability of the cyclotide kalata b1: the importance of the cyclic cystine knot. *Biochemistry*, 43(20):5965–5975, 2004.

* * *

Physics Informed Neural Networks for Solving Nonlinear Partial Differential Equations

A. Slavova, V. Ignatov

Physically Informed Neural Networks (PINNs) approximate the solutions of the PDEs by training a neural network with the aim of minimizing a loss function. It includes the terms obtained from the initial and boundary conditions along the boundary at the space-time domain, as well as at selected points in the domain.

PINNs are deep learning networks, that given a starting point in the integration domain, produce an estimated solution at that point of a differential equation after training. The inclusion of a residual network that encodes the governing physical equations is an exclusive innovation at PINNs.

The basic concept of learning with these networks is that it can be viewed as an unsupervised strategy that does not require labelled data, as a result of prior simulations and experiments. The PINNs algorithm is a unique technique that finds the solutions of the PDEs by converting the problem of directly solving the governing equations into a loss function optimization problem. It works by integrating the mathematical model into the network and strengthening the loss function with the residual term from the governing equation. PINNs take into account the main PDE, i.e. the physics of the problem rather than trying to derive a solution based solely on data, i.e. by fitting a neural network to a set of state-value pairs.

PINNs were introduced in 2017 as a new class of data-driven solvers in a two-part paper, published in a merged version subsequently in 2019 by Raissi et al. They introduce and illustrate a PINN approach for solving nonlinear PDEs, such as the Schrödinger, Burgers, and Allen-Kahn equations. They create physics-informed neural networks (PINNs) that can handle both the task of evaluating the solutions of the governing mathematical models and inverse tasks where the model parameters are learned from observable data.

PINNs have several advantages over conventional methods. They allow solutions to be differentiated using analytic gradients and provide an easy way to solve direct and inverse problems using an optimization problem. In addition to solving differential equations (a forward problem), PINNs can be used to solve inverse problems such as characterizing sensor data streams. The PINN algorithms and codes allow attacking the PDEs with very complex or high-order geometries that are difficult for numerical simulations.

In this talk we shall present the PINN solution of some nonlinear partial differential equations, as Fitzhugh Nagumo, Burgers, Fisher, etc. Numerical simulations will illustrate the theoretical results.

References

[1] Raissi, M., Karniadakis, G.E.: Hidden physics models: Machine learning of nonlinear partial differential equations. J. Comput. Phys. 357, 125–141 (2018). https://doi.org/10.1016/j.jcp.2017.11.039, www.sciencedirect.com/science/article/pii/S0021999117309014

[2] Raissi, M., Perdikaris, P., Karniadakis, G.E.: Inferring solutions of differential equations using noisy multi-fidelity data. J. Comput. Phys. 335, 736–746 (2017). DOI: 10.1016/j.jcp.2017.01.060

[3] Raissi, M., Perdikaris, P., Karniadakis, G.E.: Machine learning of linear differential equations using Gaussian processes. J. Comput. Phys. 348, 683–693 (2017). DOI: 10.1016/j.jcp.2017.07.050

[4] Raissi, M., Perdikaris, P., Karniadakis, G.E.: Physics Informed Deep Learning (Part I): Data-driven Solutions of Nonlinear Partial Differential Equations. (2017c) arXiv:1711.10561 [cs, math, stat]
[5] Raissi, M., Perdikaris, P., Karniadakis, G.E.: Physics Informed Deep Learning (Part II): Data-driven Discovery of Nonlinear Partial Differential Equations. (2017d) arXiv:1711.10566 [cs, math, stat]
[6] Raissi, M., Perdikaris, P., Karniadakis, G.E.: Numerical gaussian processes for time-dependent and nonlinear partial differential equations. SIAM J. Sci. Comput. 40(1), A172–A198 (2018). DOI: 10.1137/17M1120762
[7] Raissi,M., Perdikaris, P., Karniadakis, G.E.: Physics-informed neural networks: A deep learning framework for solving forward and inverse problems involving nonlinear partial differential equations. J. Comput. Phys. 378, 686–707 (2019). DOI: 10.1016/j.jcp.2018.10.045

* * *

Enhancing Creativity and Efficiency in Fashion with Artificial Intelligence

J. Stanchov

1 Introduction

The fashion industry, renowned for its dynamism and innovation, is undergoing significant transformation through Artificial Intelligence (AI). AI is revolutionizing design, production, and sustainability efforts, addressing critical challenges such as resource optimization and environmental impact. This paper explores the integration of mathematical and computational methods, emphasizing optimization algorithms, computer vision applications, and circular economy principles.

2 Methods and Applications

Optimization in Manufacturing Optimization algorithms such as Genetic Algorithms (GA) and Particle Swarm Optimization (PSO) are instrumental in improving resource allocation, reducing waste, and enhancing production efficiency. For example, these methods optimize fabric cutting patterns, leading to reductions of up to 40
Computer Vision for Quality Assurance AI-powered computer vision systems, leveraging convolutional neural networks (CNNs), automate quality control by detecting defects in textiles, stitching, and color patterns. This ensures superior product standards while minimizing rework and material loss.
Generative Models for Creative Processes Generative Adversarial Networks (GANs) enable designers to innovate by predicting trends and generating unique designs. This reduces prototyping time and fosters a seamless connection between designers and consumers through personalized designs.

Sustainability through Circular Economy Predictive AI models support sustainable practices by optimizing production, mitigating overproduction, and reducing waste. Additionally, AI-driven recycling systems enable automated material sorting and recovery, aligning with global sustainability goals and promoting circular fashion practices.

3 Conclusion

The integration of AI in the fashion industry marks a pivotal shift toward more creative, efficient, and sustainable practices. By combining advanced computational methods with circular economy principles, AI fosters a greener and more innovative industry. Future research should expand on AI's role in other industrial sectors facing similar sustainability challenges.

References

[1] Nayak, R., & Padhye, R. (Eds.). (2017). Automation in Garment Manufacturing. Elsevier.

* * *

Building Machine Learning Model for Handwritten Text Recognition for Analyzing the School Book 'Elementary Arithmetic' of Sava Radulov (1843)

V. Stoykova

The presentation focuses on analyzing the results of the work and performance of a Machine Learning (ML) Handwritten Text Recognition (HTR) model designed based on the text of the school book 'Elementary Arithmetic' written by Sava Radulov in 1843 in Smyrna in the Bulgarian language.

First, we offer an overview of existing approaches to HTR applied for the two major European projects that use ML to resolve the problem with text recognition to motivate the reason for using the $Transcribus$ software for our model. Later, we describe the stages of building the ML model: (i) by preprocessing text data and (ii) by processing a part of hand-transcribed data to form the Grand Truth (GT) or core ML rules. To evaluate the model performance, we use the metrics of Character Error Rate, which relates the model's output to GT, to outline the rate of HTR.

Finally, we discuss improving the ML model performance to use it further for HTR for other books in the Bulgarian language published by the same printing house in Smyrna during the period of the Revival.

* * *

Monte Carlo Techniques for Valuing Two-Dimensional European Options

V. Todorov, S. Georgiev, V. Traneva, S. Tranev

In the rapidly evolving field of financial derivatives, accurately pricing options is paramount for risk management and investment strategies. This paper introduces a comprehensive study on the application of Monte Carlo methods [1,2] to the valuation of two-dimensional European style options, which involve multiple underlying assets. The complexity of these options, due to the correlation between assets and path dependency features, makes traditional analytical approaches less effective. We explore advanced Monte Carlo techniques [2,3], including variance reduction strategies such as antithetic variates and control variates, to enhance the efficiency and accuracy of the simulation process. The paper also investigates the impact of different volatility models and correlation structures on the pricing accuracy. Through extensive computational experiments, we demonstrate that Monte Carlo methods [1], when coupled with sophisticated modeling of market conditions and intelligent implementation of variance reduction techniques, provide robust estimates that are crucial for real-world applications. The results underscore the flexibility and power of Monte Carlo simulations in handling high-dimensional and complex financial instruments.

References

[1] Wilmott, P., Dewynne, J., Howison, S.: OptionPricing:Mathematical ModelsandComputation, Oxford UniversityPress (1995).

[2] Duffie, D.: SecurityMarkets:StochasticModels,AcademicPress, Inc. (1988).

[3] Dimov, I.: Monte Carlo Methods forApplied Scientists, NewJersey, London, Singapore, WorldScientific (2008).

* * *

Advanced Monte Carlo Approaches for Extensive Sensitivity Analysis

V. Todorov, S. Georgiev, V. Traneva, S. Tranev, M. Petrov

Sensitivity analysis is an indispensable tool across various scientific disciplines, providing insights into the influence of input variability on output in mathematical models and simulations. This process is crucial for understanding system behavior, enhancing model predictions, optimizing design parameters, and supporting decision-making processes under uncertainty. Advanced Monte Carlo methods, characterized by their stochastic nature, have emerged as a powerful approach to conduct sensitivity analysis, especially for complex, nonlinear, or multidimensional systems where traditional analytical methods fall short [1]. Monte

Carlo approach not only accommodates models with a high degree of non-linearity and interaction effects but also handles large parameter spaces with ease. Furthermore, the Monte Carlo method offers the flexibility to integrate with various variance-based sensitivity analysis techniques, such as Sobol indices, which quantify each input's contribution to the output variance.

This paper aims to delve into the development and application of advanced Monte Carlo techniques for sensitivity analysis [1,2]. It discusses the integration of these methods with contemporary computational tools and statistical techniques to enhance the accuracy, efficiency, and interpretability of sensitivity analysis results. The focus will be on novel adaptations based on the use of lattice and digital sequences to efficiently estimate the Sobol' sensitivity indices.

References

[1] Todorov, V., Georgiev, S., Georgiev, I., Traneva, V., Tranev, S.: Multidimensional Air Pollution Sensitivity Analysis for Intelligent Decision Modeling by Means of Quasi-Monte Carlo Sequences. In: Kahraman, C., Cevik Onar, S., Cebi, S., Oztaysi, B., Tolga, A.C., Ucal Sari, I. (eds) Intelligent and Fuzzy Systems. INFUS 2024. Lecture Notes in Networks and Systems, vol. 1090. Springer, Cham. https://doi.org/10.1007/978-3-031-67192-0_36

[2] Dimov, I., Georgieva, R., Ivanovska, S., Ostromsky, Tz., Zlatev, Z.:Studying the sensitivity of pollutants' concentrations caused by variations of chemical rates, Journal of Computational and Applied Mathematics **235** (2), 391-402 (2010). https://doi.org/10.1016/j.cam.2010.05.041

* * *

Reference pseudonymization model for medical information systems

T. Tsokov, H. Kostadinov

A Medical Information System (MIS) is composed of hardware, software, data and operations to provide functionality related to user's health in healthcare organization. This functionality should span across short and long periods of time. The data contains sensitive user information, so its security aspects like confidentiality, integrity and availability are important. There are a lot of technical challenges in order to implement secure and reliable MIS. On the other hand there are no systematic guidelines and standards for implementation of the data security part. We are presenting a reference model and architecture for data pseudonymization in MIS, which can serve as an implementation guideline. It exposes several configuration parameters depending on the data, functionality and time period.

References

[1] He Zhicheng: From Privacy-Enhancing to Health Data Utilization: The Traces of Anonymization and Pseudonymization in EU Data Protection Law. Digital Society 2, 69-78 (2023). DOI: 10.1007/s44206-023-00043-5

[2] Keikhosrokiani P.: Chapter 16 - System development for different information systems. Perspectives in the Development of Mobile Medical Information Systems: Life Cycle, Management, Methodological Approach and Application, 259-268 (2020). DOI: 10.1016/B978-0-12-817657-3.00016-X
[3] Sajedi H., Yaghobi S.R.: Information hiding methods for E-Healthcare. Smart Health, vol. 15, 100104 (2020). DOI: 10.1016/j.smhl.2019.100104

* * *

Useful configurations in STS(v) of small order

A. Tsvetanova, S. Zhelezova

A Steiner triple system of order v (STS(v)) is a pair (V, B) where V is a v-element set and B is a family of 3-element subsets of V called blocks such that each pair of elements of V is contained in exactly one block of B. An STS(v) is cyclic if it has a cyclic automorphism group of order v.
An (m, n)-configuration in an STS(v) is a set of n distinct triples which cover together m points. An STS(v) is l-sparse if it doesn't contain any $(i + 2, i)$-configurations for $i \leq l$. Each l-sparse STS(v), $l > 2$, is also $(l - 1)$-sparse. Up to now most of the l-sparse STS(v) constructions pay attention on the unique Pasch ((6,4)-configuration) and the unique mitre ((7,5)-configuration) configuration.
The cyclic STS(v)s are important because of their close connection to the binary (k, r)-regular quasi-cyclic LDPC codes [1]. The LDPC codes based on cyclic STS(v)s can have a high rate and a relatively short length. The lack of the Pasch configurations in the cyclic STS(v) implies that the minimum distance of the corresponding LDPC code is six instead of four [2].
The STS(v)s with the maximal possible number of Pasch configurations are also important for example in connection to a Steiner loop. There is a one-to-one correspondence between an STS(v) and a nontrivial Steiner loop of order $v+1$. A Steiner loop with a nontrivial center corresponds to an STS(v) with a large number of Pasch configurations [3].
An STS(v) is 4-sparse (anti-Pasch) iff it doesn't contain any Pasch configuration. The 4-sparse STS(v) exist for every $v \equiv 1, 3 \pmod 6$ except for $v \in \{7, 13\}$ [4].
An STS(v) is anti-mitre iff it doesn't contain any mitre configuration. An STS(v) is 5-sparse iff it is both anti-Pasch and anti-mitre. The 5-sparse STS(v) has been subject to active research. One of the first infinite classes of 5-sparse STS(v) includes Netto systems of order 19 (mod 24)[5]. In the same paper the existence of transitive 5-sparse STS(v), $v = 19$, $33 \leq v \leq 97$ [5] is established. A 5-sparse STS(v) also exists for $v \equiv 1,\ 19 \pmod{54}$, $v \neq 109$ [6]. Recently constructions of 5-sparse STS(v) for all $v \equiv 3 \pmod 6$ and $v \geq 21$ are presented in [7] and the author proved that 5-sparse STS(v) exists for almost all possible orders.
Up to this work the number of the anti-Pasch, anti-mitre and 5-sparse cyclic STS(v) of orders up to 57 were known [5]. Here we present the 4 and 5-sparse cyclic STS(61)s. There are

42373196 cyclic STS(61)s [8]. Our computer results show that 2630618 of them are 4-sparse (anti-Pasch) 199749 are anti-mitre and 9309 are 5-sparse.
We also consider the number of the Pasch and the mitre configurations in the cyclic STS(v)s of orders up to 61 (not only the cases when they are missing). This together with some theoretical results from [5] allow us to improve some of the lower bounds for the maximal number of Pasch configurations in an STS(v), $v \leq 61$. In addition our computational results can serve as the lower bounds for the maximal number of the mitre configurations in the STS(v), $v \leq 61$.

Acknowledgments The research is partially supported by the Bulgarian National Science Fund under Contract No KP-06-H62/2-2022.

References

[8] T. Baicheva, S. Topalova. Classification results for (v, k, 1) cyclic difference families with small parameters, Mathematics of Distances and Applications. M. Deza, M. Petitjean, K. Markov (Eds.), in International book series: Information Science and Computing, 25 (2012), 24–30.
[5] C. Colbourn, E. Mendelsohn, A. Rosa, J. Siran. Anti-Mitre Steiner Triple Systems, Graphs Comb. 10 (1994), 215–224.
[6] Y. Fujiwara. Infinite classes of anti-mitre and 5-sparse Steiner triple systems, J. Combin. Des. 14 (2006), 237–250.
[4] M. J. Grannell, T. S. Griggs, C. A. Whitehead. The resolution of the anti-Pasch conjecture, J. Combin. Des. 8 (4) (2000)300–309.
[1] A. Gruner, M. Huber. New combinatorial construction techniques for low-density parity-check codes and systematic repeat-accumulate codes, IEEE Trans. Commun. 60(9) (2012) 2387–2395.
[3] A. Kozlik. The centre of a Steiner loop and the maxi-Pasch problem, Comment. Math. Univ. Carolin. 61 (4) (2020), 535–545.
[2] B. Vasic, O. Milenkovic. Combinatorial constructions of low-density parity-check codes for iterative decoding, IEEE Trans. Inform. Theory 50 (2004), 1156–1176.
[7] A. Wolfe. The existence of 5-sparse Steiner triple systems of order $n \equiv 3$ mod 6, $n \neq \{9,15\}$, J. Combin. Theory Ser. A 115 (8) (2008), 1487–1503.

* * *

Interpolation of Convex Scattered Data in $\mathbb{R}^3$ using Edge Convex Minimum L_p-Norm Networks, $1 < p < \infty$

K. Vlachkova

Interpolation of scattered data in $\mathbb{R}^3$ is a fundamental problem in applied mathematics and finds applications in various fields such as computer graphics and animation, scientific visualization, medicine (computer tomography), automotive, aircraft and ship design, architecture, archaeology, and many more. Various methods for solving this problem were proposed and applied. Nielson [1] set and solved the extremal problem of interpolation of scattered data in

$\mathbb{R}^3$ using smooth curve networks with minimal L_2-norm of the second derivative which are defined on the edges of an associated triangulation. Andersson et al. [2] gave a novel proof of Nielson's result which allowed them to consider and handle the case where the data are convex and we seek a convex interpolant. Andersson et al. formulate and solve the corresponding extremal constrained interpolation problem of finding a minimum norm network that is convex along the edges of the triangulation. Vlachkova [3] extended the results in [1, 2] and solved the extremal unconstrained problem (without convexity constraint) of interpolation of scattered data by minimum L_p-norms networks for $1 < p < \infty$. Here we present a comprehensive solution to the constrained extremal problem of interpolation of convex scattered data in $\mathbb{R}^3$ using smooth curve networks with minimal L_p-norm of the second derivative, $1 < p < \infty$, while ensuring convexity along the edges of the associated triangulation. The solution to the problem is unique in the case of strictly convex data and is obtained from the solution to a nonlinear system of equations determined by the data. Our results allow the efficient computation of the solutions to the constrained problem for $1 < p < \infty$. Numerical experiments are presented and visualized to illustrate and support our results. The computation and visualization are obtained using Wolfram Mathematica package.

Example 1 *The data are sampled for* $n = 30$ *from the convex function* $f(x, y) = -\ln^2\left(16 - (x-3)^2 - (y - 3\sqrt{3}/2)^2\right)$. *We consider the case* $p = 2$. *The triangulation* T *and the corresponding edge convex minimum* L_2*-norm network are shown in Fig. 1.*

Example 2 *The data are obtained from a regular triangular pyramid. They are* $P_1 = (-1/2, -\sqrt{3}/6, 0)$, $P_2 = (1/2, -\sqrt{3}/6, 0)$, $P_3 = (0, \sqrt{3}/3, 0)$, *and* $P_4 = (0, 0, -1/2)$. *The triangulation* T, *the edge convex minimum* L_p*-norm networks* F_p *with the corresponding* L_p*-norms* $\|F_p''\|_p$ *for* $p = 1.5,\ 2,\ 3,\ 6$, *and the edge convex minimum* L_∞*-norm network* F^* *(see [4]) are shown in Fig. 2.*

Acknowledgments This work was supported in part by Sofia University Science Fund Grant No. 80-10-156/2024.

Figure 1: Example 1: The triangulation T and the corresponding edge convex minimum L_2-norm network for $n = 30$ and $p = 2$.

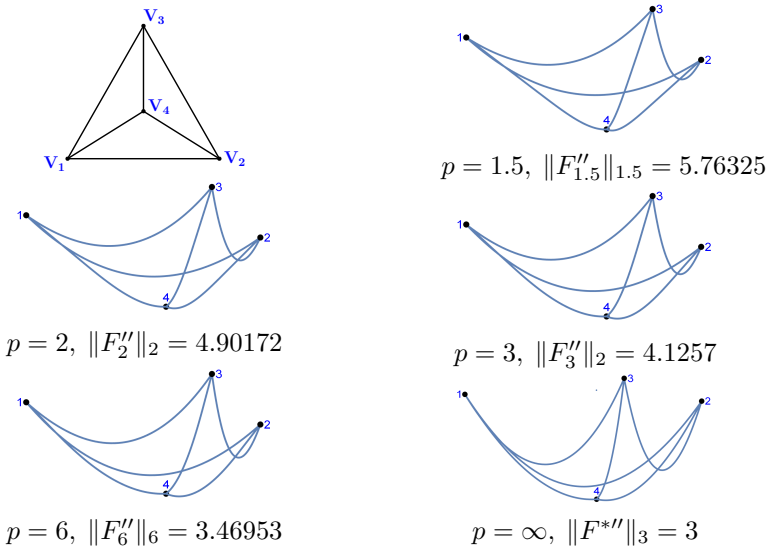

Figure 2: Example 2: The triangulation T, the edge convex minimum L_p-norm networks F_p with the corresponding L_p-norms $\|F_p''\|_p$ for $p = 1.5,\ 2,\ 3,\ 6$, and the edge convex minimum L_∞-norm network F^*.

References

[1] G. M. Nielson. A method for interpolating scattered data based upon a minimum norm network. *Math. Comp.*, 40(161), 253-271, 1983. DOI: 10.1090/S0025-5718-1983-0679444-7

[2] L.-E. Andersson, T. Elfving, G. Iliev, K. Vlachkova. Interpolation of convex scattered data in $\mathbb{R}^3$ based upon an edge convex minimum norm network. *J. Approx. Theory*, 80(3), 299-320, 1995. DOI: 10.1006/jath.1995.1020

[3] K. Vlachkova, Interpolation of scattered data in $\mathbb{R}^3$ using minimum L_p-norm networks, $1 < p < \infty$, *J. Math. Anal. Appl.*, 482, 123824, 2020. DOI: 10.1016/j.jmaa.2019.123824

[4] K. Vlachkova, Extremal interpolation of convex scattered data in $\mathbb{R}^3$ by smooth edge convex minimum L_∞-norm networks: Characterization and solution, *Math. Methods Appl. Sci.*, 2024. DOI: 10.1002/mma.10543.

* * *

Algorithmic trading: Automated Volume Spread Analysis for Identification of Trend Reversals

P. Zhivkov

In algorithmic trading, systematic, data-driven models guide trade execution, enabling traders to capitalize on high-frequency or non-standard market conditions. This study applies Volume Spread Analysis (VSA) to cryptocurrency markets, aiming to enhance algorithmic trading strategies by analyzing the relationship between trading volume and price spread. VSA posits that volume should typically confirm price movement, meaning that higher volumes accompany larger price movements (high spreads), while lower volumes align with narrower ranges. However, significant deviations from this relationship often highlight unusual market dynamics, offering critical insights into potential trend reversals or consolidation phases.

1 Introduction

Algorithmic trading is an essential evolution in modern financial markets, driven by advancements in computing power and the availability of high-quality, high-frequency data. Traditional manual trading, which relies on interpreting market signals based on time-lagged information and often subjective analysis, has limitations in fast-paced, complex markets like cryptocurrencies. By leveraging algorithms to systematically detect and act on volume-spread anomalies in real-time, traders can significantly enhance decision-making speed, accuracy, and consistency.

2 Implementation of an Adaptive Predictive Model

To move beyond static categorizations, this study employs an adaptive rolling linear regression model that calculates the expected price spread based on recent volume data. Using a rolling window of 168 candles, the model adjusts continuously to recent market conditions, using volume as the independent variable and price spread as the dependent variable. This dynamic framework allows for real-time adjustments and generates a baseline ”expected” spread for each new data point. The difference between actual and predicted spread values is treated as an indicator: a positive deviation suggests an unexpectedly wide price range given the current volume, while a negative deviation suggests a narrow price range despite substantial trading volume. The model is designed to identify points where the relationship between volume and spread deviates significantly from expected values, signaling potential market inefficiencies. A high deviation from the predicted spread may highlight critical moments in price action where traditional trend-following indicators might fail to capture the true sentiment due to liquidity imbalances.

3 Applications and Implications

The proposed VSA-based indicator can be particularly valuable in identifying non-traditional trading setups by focusing on outlier scenarios (i.e., high volume with low spread and low volume with high spread). Practical use cases include:

- Trend Reversal Detection: Instances of high volume with low spread are commonly observed near trend reversals, where large market participants might be absorbing liquidity to prevent further price escalation or decline. By detecting this pattern, traders can anticipate potential trend changes before conventional indicators reflect the shift.
- Breakout and Consolidation Signals: Low volume with high spread can be a hallmark of liquidity-driven price shifts, often occurring in low-interest periods. This indicator can help traders avoid "false breakouts" or anticipate a return to equilibrium as liquidity normalizes.
- Risk Management: By flagging atypical volume-spread relationships, this indicator allows traders to exercise greater caution during periods of market imbalance, thus aiding in risk management and avoiding low-probability trades.

4 Conclusion

This research establishes the foundation for applying an adaptive VSA model in cryptocurrency markets, particularly for BTC-USD, ETH-USD, and DOGE-USD pairs. Our findings suggest that systematically capturing and analyzing volume-spread deviations provides a nuanced perspective on market behavior, particularly in identifying non-standard conditions that could mark turning points or periods of market consolidation. Further research could extend this approach to a broader set of digital assets and explore machine learning enhancements for real-time adaptability and precision.

* * *

Part B

List of participants

Todorka Alexandrova
Institute of Mathematics and Informatics
Bulgarian Academy of Sciences
Acad. G. Bonchev Str., Bl. 8
1113 Sofia, Bulgaria
toty@math.bas.bg

Todor Balabanov
Institute of Information and
Communication Technologies
Bulgarian Academy of Sciences
Acad. G. Bonchev Str, Bl. 2
1113 Sofia, Bulgaria
todor.balabanov@gmail.com

Milen Borisov
Institute of Mathematics and Informatics
Bulgarian Academy of Sciences
Acad. G. Bonchev str., bl. 8
1113 Sofia, Bulgaria
milen_kb@math.bas.bg

Gergana Chalakova
Institute of Mechanics
Bulgarian Academy of Sciences
Acad. G. Bonchev Str., Bl. 4
1113 Sofia, Bulgaria
Gergana Chalakova

Maria Datcheva
Institute of Mechanics
Bulgarian Academy of Sciences
Acad. G. Bonchev Str., Bl. 4
1113 Sofia, Bulgaria
datcheva@imbm.bas.bg

Hristo Djidjev
Institute of Information and
Communication Technologies
Bulgarian Academy of Sciences
Acad. G. Bonchev Str., bl. 25A
1113 Sofia, Bulgaria
hdjidjev@msn.com

Jordan Genoff
Technical University of Sofia, branch Plovdiv
63 Sankt Peterburg Blvd.
4000 Plovdiv, Bulgaria
jgenoff@tu-plovdiv.bg

Ivan Georgiev
Institute of Information and
Communication Technologies
Bulgarian Academy of Sciences
Acad. G. Bonchev Str., Bl. 2
1113 Sofia, Bulgaria
john.g.georgiev@gmail.com

Slavi Georgiev
Ruse University “Angel Kanchev”
8 Studentska Str.
7017 Ruse, Bulgaria
iivanova@geophys.bas.bg

Irina Georgieva
Institute of Mathematics and Informatics
Bulgarian Academy of Sciences
Acad. G. Bonchev Str., Bl. 8
1113 Sofia, Bulgaria
irina@math.bas.bg

Stanislav Harizanov
Institute of Information and
Communication Technologies &
Institute of Mathematics and Informatics,
Bulgarian Academy of Sciences
Acad. G. Bonchev Str., bl. 25A
1113 Sofia, Bulgaria
sharizanov@parallel.bas.bg

Roumen Iankov
Institute of Mechanics
Bulgarian Academy of Sciences
Acad. G. Bonchev Str., Bl. 4
1113 Sofia, Bulgaria
iankovr@abv.bg

Nevena Ilieva
Institute of Information and
Communication Technologies
Bulgarian Academy of Sciences
Acad. G. Bonchev Str, Bl. 25A
1113 Sofia, Bulgaria
nevena.ilieva@iict.bas.bg
and
Institute of Mathematics and Informatics
Bulgarian Academy of Sciences
Acad. G. Bonchev Str., Bl. 8
1113 Sofia, Bulgaria

Veselina Ivanova
Faculty of Physics
Sofia University "St. Kl. Ohridski"
5 J. Bourchier Blvd.
1164 Sofia, Bulgaria
veselina559@gmail.com

Miglena Koleva
Ruse University
6 Studentska St
7017 Ruse, Bulgaria
mkoleva@uni-ruse.bg

Hristo Kostadinov
Institute of Mathematics and Informatics
Bulgarian Academy of Sciences
Acad. G. Bonchev str., bl. 8
1113 Sofia, Bulgaria
hristo@math.bas.bg

Elena Lilkova
Institute of Information and
Communication Technologies
Bulgarian Academy of Sciences
Acad. G. Bonchev Str., Bl. 25A
1113 Sofia, Bulgaria
elena.lilkova@iict.bas.bg

Józef Adam Liwo
University of Gdańsk
ul. Wita Stwosza 63
80-308 Gdańsk, Poland
adam.liwo(at)ug.edu.pl

Zlatogor Minchev
Institute of Information and
Communication Technologies
Bulgarian Academy of Sciences
Acad. G. Bonchev Str., Bl. 25A
1113 Sofia, Bulgaria
zlatogor@bas.bg

Tzvetan Ostromsky
Institute of Information and
Communication Technologies
Bulgarian Academy of Sciences
Acad. G. Bonchev Str., Bl. 25A
1113 Sofia, Bulgaria
ceco@parallel.bas.bg

Maria Pashinska-Gadzheva
Institute of Mathematics and Informatics
Bulgarian Academy of Sciences
Acad. G. Bonchev str., bl. 8
1113 Sofia, Bulgaria
mariqpashinska@math.bas.bg

Peicho Petkov
Faculty of Physics
Sofia University "St. Kl. Ohridski"
5 J. Bourchier Blvd.
1164 Sofia, Bulgaria
peicho@phys.uni-sofia.bg

Milan Rashevski
Institute of Mechanics
Bulgarian Academy of Sciences
Acad. G. Bonchev Str.,Bl. 4
1113 Sofia, Bulgaria
mrashevski@gmail.com

Miglena Raykovska
Institute of Information and
Communication Technologies
Bulgarian Academy of Sciences
Acad. G. Bonchev Str., Bl. 2
1113 Sofia, Bulgaria
miglena.raykovska@iict.bas.bg

Miryana Raykovska
Institute of Information and
Communication Technologies
Bulgarian Academy of Sciences
Acad. G. Bonchev Str., Bl. 2
1113 Sofia, Bulgaria
mirianaraykovska@gmail.com

Elton Shumka
Faculty of Physics
Sofia University "St. Kl. Ohridski"
5 J. Bourchier Blvd.
1164 Sofia, Bulgaria
elton.shumka@cern.ch

Petya Sirakova
Faculty of Physics
Sofia University "St. Kl. Ohridski"
5 J. Bourchier Blvd.
1164 Sofia, Bulgaria
sirakovapetya@gmail.com

Angela Slavova
Institute of Mechanics
Bulgarian Academy of Sciences
Acad. G. Bonchev Str., Bl. 4
1113 Sofia, Bulgaria
angela.slavova@gmail.com

Jelenko Stanchov
Institute of Information and
Communication Technologies
Bulgarian Academy of Sciences
Acad. G. Bonchev Str, Bl. 25A
1113 Sofia, Bulgaria
elenko.stanchov@iict.bas.bg

Velislava Stoykova
Institute for the Bulgarian Language
"Prof. Lyubomir Andreychin"
Bulgarian Academy of Sciences
52 Shipchensky prohod Blvd, Bl. 17
1113 Sofia, Bulgaria
vstoykova@yahoo.com

Stefan Tafkov
Institute of Information and
Communication Technologies
Bulgarian Academy of Sciences
Acad. G. Bonchev Str., Bl. 25A
1113 Sofia, Bulgaria
stefan.k.tafkov@gmail.com

Ilian Todorov
STFC Scientific Computing
Keckwick Lane
Daresbury, UK
ilian.todorov@stfc.ac.uk

Venelin Todorov
Institute of Information and
Communication Technologies
Bulgarian Academy of Sciences
Acad. G. Bonchev Str, Bl. 25A
1113 Sofia, Bulgaria
venelinltodorov@gmail.com
and
Institute of Mathematics and Informatics
Bulgarian Academy of Sciences
Acad. G. Bonchev Str., Bl. 8
1113 Sofia, Bulgaria

Stoyan Tranev
"Prof. Asen Zlatarov" University
"Prof. Yakimov" Blvd 1
8000 Burgas, Bulgaria

Velichka Traneva
"Prof. Asen Zlatarov" University
"Prof. Yakimov" Blvd 1
8000 Burgas, Bulgaria

Tsvetan Tsokov
Institute of Mathematics and Informatics
Bulgarian Academy of Sciences
Acad. G. Bonchev str., bl. 8
1113 Sofia, Bulgaria
tsvetan.tso@gmail.com

Antoaneta Tsvetanova
Institute of Mathematics and Informatics
Bulgarian Academy of Sciences
Acad. G. Bonchev Str., Bl. 8
1113 Sofia, Bulgaria
a.cvetanova@math.bas.bg

Nikolay K. Vitanov
Institute of Mechanics
Bulgarian Academy of Sciences
Acad. G. Bonchev Str.,Bl. 4
1113 Sofia, Bulgaria
vitanov@imbm.bas.bg

Georgi Vasilev
Institute of Information and
Communication Technologies
Bulgarian Academy of Sciences
Acad. G. Bonchev Str., Bl. 2
1113 Sofia, Bulgaria
electropioneer@mail.bg

Krassimira Vlachkova
Faculty of Mathematics and Informatics
Sofia University "St. Kl. Ohridski"
5 J. Bourchier Blvd.
1164 Sofia, Bulgaria
krassivl@fmi.uni-sofia.bg

Lubin Vulkov
Ruse University
6 Studentska St
7017 Ruse, Bulgaria
lvalkov@uni-ruse.bg

Stela Zhelezova
Institute of Mathematics and Informatics
Bulgarian Academy of Sciences
Acad. G. Bonchev Str., Bl. 8
1113 Sofia, Bulgaria
stela@math.bas.bg

Petar Zhivkov
Institute of Information and
Communication Technologies
Bulgarian Academy of Sciences
Acad. G. Bonchev Str, Bl. 25A
1113 Sofia, Bulgaria
zhivkovpetar@gmail.com